13

Structural and phase analysis of the Ge(111)$c(2 \times 8)$, Si(100)(2×1) and BaO/Si(100) surfaces by means of height histograms in scanning tunneling microscopy

© M.V. Kuzmin, D.A. Malkov

Ioffe Institute, St. Petersburg, Russia
E-mail: m.kuzmin@mail.ioffe.ru

Received February 3, 2025
Revised February 3, 2025
Accepted March 2, 2025

We demonstrate that quantitative analysis of topography height distributions in scanning tunneling microscopy may be utilized to probe not only the surface roughness but also the atomic arrangement, morphological structure, and phase composition of various samples. The implementation of such analysis is reported for well-known model surfaces, such as Ge(111)$c(2 \times 8)$ and Si(100)(2×1), as well as BaO/Si(100) thin-film system, prepared at different temperatures.

Keywords: scanning tunneling microscopy, surface morphology, height histogram, atomic structure, phase composition.

DOI: 10.61011/TPL.2025.06.61285.20272

In scanning tunneling microscopy (STM), the most often chosen test objects are surfaces characterized by long-range order or regularly repeating features in the form of vacancies, steps, clusters, atomic chains, nanowires, etc. It is possible to obtain for them not only a map of the local density of states, but also other important data concerning, e.g. interaction of steps [1], mass transfer phenomena [2], Friedel oscillations [3], surface reactions [4], kinetics and energetics of atomic processes [5,6]. At the same time, STM is believed to be less informative for surfaces having no regular structure, for instance for amorphous films. In this case, only roughness parameters are typically assessed, e.g. average surface profile height, standard deviation, asymmetry (skewness) and kurtosis of the height distribution.

The goal of this study was to show that quantitative analysis of topography, namely STM height histograms, can provide much more valuable information than the above-mentioned topographic characteristics. For instance, those histograms contain information about the atomic arrangement, morphological structure and phase composition of crystalline and amorphous surfaces. The experiments were conducted using ultrahigh vacuum microscope Omicron STM 1 operating at room temperature. Images obtained with it were recorded in the constant current mode. Tips were made of tungsten. As substrates, Si(100)(2×1) and Ge(111)$c(2 \times 8)$ surfaces were used. They were cleaned by short-term heating at the temperatures of 1200 to 1230 °C (for silicon) or by bombarding with 1.0 keV Ar^+ ions with subsequent annealing at 630 °C (for germanium).

STM images obtained in the constant current mode nothing else but sets of the $z(x, y)$ values, namely, tip vertical positions (heights) at the surface points with Cartesian coordinates x and y. These data may be represented as height distribution histograms $F(z)$ illustrating the z values repetition rate on the selected sample area. In the simplest case of an ideal structureless surface, such a distribution has the form of a delta function. That for a real surface may be represented as a linear combination of several functions $f_i(z)$ describing the height distributions for each unit cell's building block, i.e. $F(z) = \sum_i f_i(z)$. If the surface is formed not by one but by several phases, the height histogram is represented as $F(z) = F_1(z) + F_2(z) + \ldots F_n(z)$, where n is the number of phases. It follows from the above that, by analyzing the $F(z)$ shape and decomposing the curve into individual components, it is possible to obtain data on the surface structure even when its direct visualization in the STM image is impossible. Now consider some specific cases.

Fig. 1, *a* shows an image of the Ge(111)$c(2 \times 8)$ surface with atomic resolution in the mode of unfilled states. Its geometric and electronic structures were studied in detail previously [7]. Protrusions in the given image (density of states maxima) are located near the so-called adatoms (designated as A), i.e. Ge atoms that form the upper layer of reconstruction $c(2 \times 8)$. Troughs (density of states minima) are located near rest atoms (R) or atoms localized in the second reconstruction layer and forming no bonds with adatoms. On the right of Fig. 1, *a*, height histogram corresponding to the considered image is presented. For the ease of perception, the results are represented not in the form of columns but by dots (circles). The presented dependence has a rather complex asymmetric shape. As the analysis has shown, it is constituted by at least three components, that is, Gaussian peaks. Peaks A and R at $z = 1.51$ and 0.76 Å are generated by adatoms and rest atoms, respectively. Peak S observed at intermediate heights corresponds to surface areas between protrusions

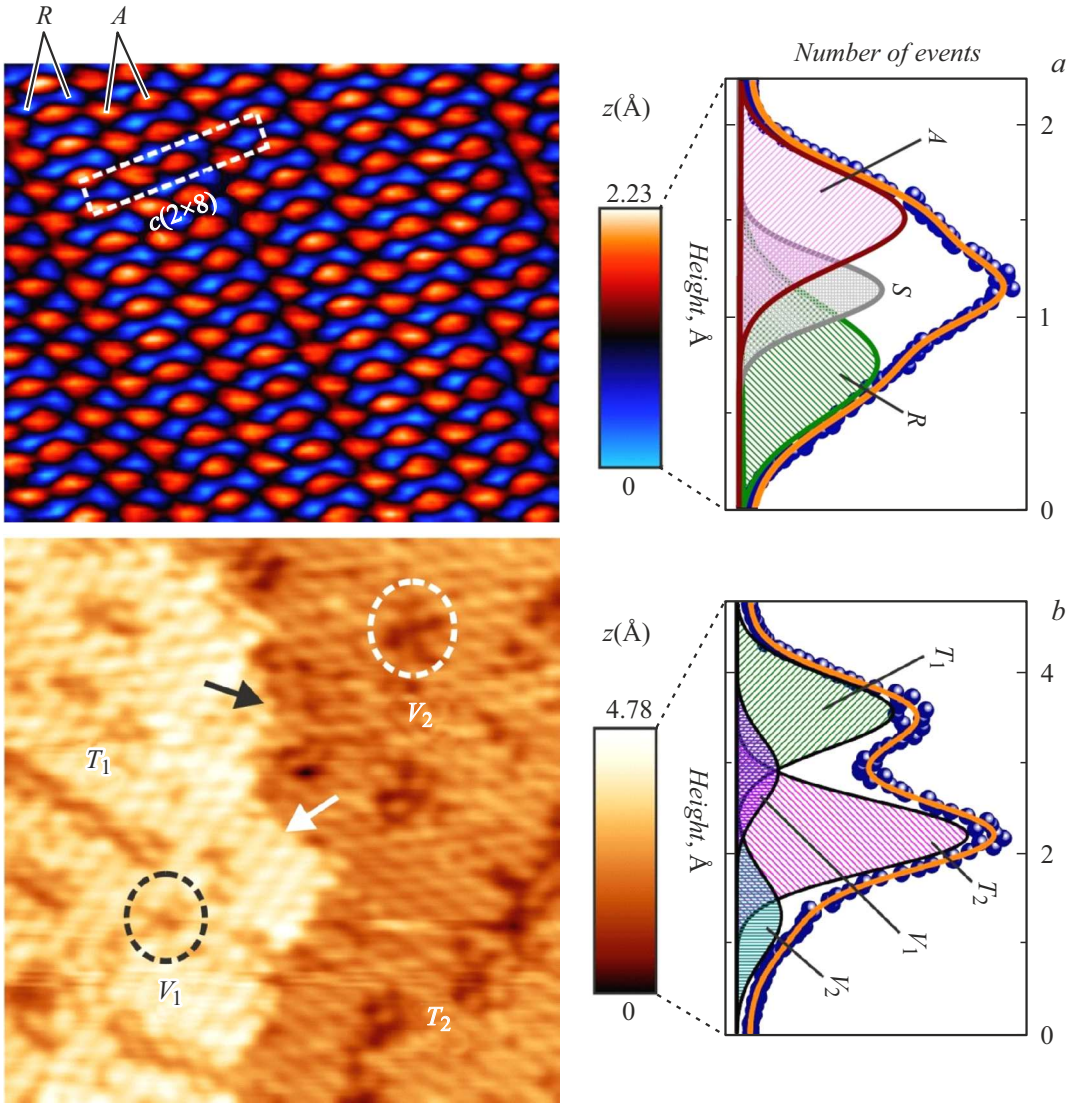

Figure 1. STM images (left panels) and height histograms (right panels) for the Ge(111)$c(2 \times 8)$ (*a*) and Si(100)(2×1) (*b*) surfaces. Bias voltage (the tip-sample potential difference), tunneling current and image size are, respectively: *a* — 2.0 V, 0.98 nA, 7.8×6.4 nm; *b* — 1.9 V, 0.18 nA, 16.4×16.7 nm. In the histograms (columns are not shown) dots represent the height distributions, while solid lines represent the results of distribution fitting. See the text for details.

and troughs. The distance from maximum A to R along the z axis is 0.75 Å. This distance matches the difference in vertical positions of adatoms and rest atoms [7]. Also noteworthy is the approximate equality of the areas of peaks R and A. This correlates with the quantitative ratio (1:1) between adatoms and rest-atoms in the $c(2 \times 8)$ cell. All this means that analysis of the shape of the curve on the surface topography height histogram can provide detailed information on features of its atomic arrangement.

The germanium surface area shown in Fig. 1, *a* is atomically smooth and does not contain steps, defects, or so on. Obviously, complication of the morphological structure is expected to cause relevant variations in the height histogram. For instance, when a local cluster is formed on the Ge(111)$c(2 \times 8)$ reconstruction, the height distribution curve has two maxima (not shown). One of them that is shifted towards lower z may be attributed to uncoated surface $c(2 \times 8)$, while the other shifted to higher z is caused by the three-dimensional cluster.

Another case illustrating interrelation between the height-histogram curve type and surface morphological structure are the results shown in Fig. 1, *b*. The figure demonstrates the Si(100)(2×1) surface topography with two terraces separated by a monatomic-height step (indicated by arrows). In addition, the STM image exhibits on the terraces local dark areas (troughs). They are marked with ovals. These are natural vacancies spontaneously arising to reduce surface tension in the silicon dimer rows of the (2×1) structure [8]. All the mentioned features are reflected in the height histogram presented in Fig. 1, *b*. The presented dependence

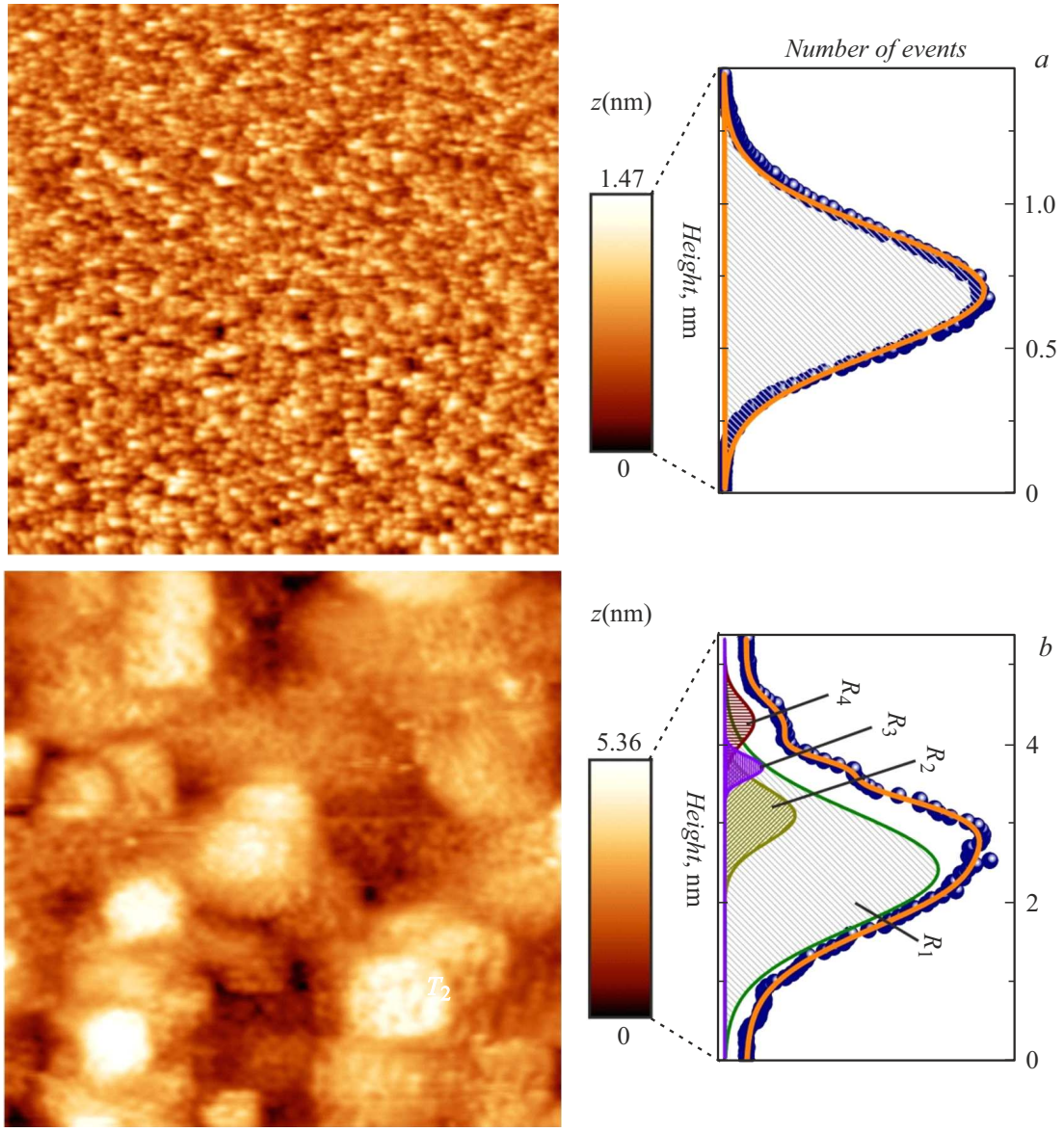

Figure 2. The same as in Fig. 1 but for the BaO/Si(100) film systems formed at room temperature (a) and at 580 °C (b). Parameters at which STM images were obtained are as follows: a — 2.2 V, 0.01 nA, 160 × 160 nm; b — 4.0 V, 0.18 nA, 270 × 270 nm.

includes four components. Two of them (T_1 and T_2) are caused by regular structure (2×1) on the upper and lower terraces. The distance between those components is $\Delta z = 1.35$ Å, which is almost equal to the step height. The other two components (V_1 and V_2) are associated with vacancies on both terraces. The ratio between intensities of maxima T_1, T_2, V_1 and V_2 is 3.8 : 5.5 : 1 : 1.3, which approximately matches the ratio of areas occupied by the relevant features of the STM image.

A distinctive feature of the STM images shown in Fig. 1 is that they can provide a clear view of structural properties of the surfaces under study even without height histograms. The situation becomes more complicated when there is no image ordering. In this case, properties of the object under study may be clarified by height histograms. Fig. 2 demonstrates the results for the barium monoxide films grown on Si(100). This compound has a simple cubic lattice of the NaCl type, is a *high-k* dielectric, and is of practical interest as a candidate for replacing insulating SiO_2 layers in MOSFET transistors [9]. In this study, epitaxial BaO layers were obtained on a silicon substrate at room temperature by the method proposed in [10]. The films' long-range order was confirmed by low-energy electron diffraction. Fig. 2, *a* shows an STM image of the crystalline BaO film 8 nm thick. Evidently, the film roughness is fairly low; however, its surface exhibits no regular structure. The height histogram of this film has a form of the normal (Gaussian) distribution which may be representes by a single component. This gives reasons for assuming that the film is chemically

homogeneous and does not contain any other phases except for barium monoxide.

The BaO film properties change radically after heating at 580 °C. This transformation is visible, first of all, in the STM image (Fig. 2, *b*). However, even more significant changes are observed in the height histogram which gets a considerably more complex shape than at room temperature and includes minimum four components (R_1–R_4). This evidences that the heated film becomes multiphase. Indeed, data of [10] show that at the mentioned temperature atoms diffuse from the silicon substrate into the film, which leads to formation of several silicate-like compounds $BaSi_xO_y$. What are noteworthy are positions of the R_2–R_4 peaks on the histogram height scale. Apparently, phases corresponding to them tend to segregate on the film structure surface. Thus, the results presented in Fig. 2 show that STM height histograms may be used in studying phase compositions of various film systems.

Note in conclusion that the issue of selecting a model function for fitting height histograms is beyond the scope of this paper and is not, therefore, discussed in detail. It is known that the Gaussian (normal) distribution (as well as a mixture of normal distributions) is used in many tasks of data analysis in physics, biology, mechanical engineering, economics and finance [11,12]. In addition to the Gaussian function, we have studied in this work other, more complex functions, e. g. the Voigt profile. The results obtained in this case did not differ qualitatively from those presented above.

Conflict of interests

The authors declare that they have no conflict of interests.

References

[1] L. Persichetti, A. Sgarlata, M. Fanfoni, M. Bernardi, A. Balzarotti, Phys. Rev. B, **80**, 075315 (2009). DOI: 10.1103/PhysRevB.80.075315
[2] Y.P. Zhang, K.S. Yong, H.S.O. Chan, G.Q. Xu, S. Chen, X.S. Wang, A.T.S. Wee, Phys. Rev. B, **75**, 073407 (2007). DOI: 10.1103/PhysRevB.75.073407
[3] K. Sotthewes, M. Nijmeijer, H.J.W. Zandvliet, Phys. Rev. B, **103**, 245311 (2021). DOI: 10.1103/PhysRevB.103.245311
[4] P.J. Keenan, R.M. Purkiss, T. Klamroth, P.A. Sloan, K.R. Rusimova, Nat. Commun., **15**, 10322 (2024). DOI: 10.1038/s41467-024-54677-1
[5] X.-Y. Ren, C.-Y. Niu, W.-G. Chen, M.-S. Tang, J.-H. Cho, Phys. Chem. Chem. Phys., **18**, 18549 (2016). DOI: 10.1039/C6CP01919F
[6] O. Ochs, N. Martsinovich, W.M. Heckl, M. Lackinger, J. Phys. Chem. Lett., **11**, 7320 (2020). DOI: 10.1021/acs.jpclett.0c01882
[7] N. Takeuchi, A. Selloni, E. Tosatti, Phys. Rev. Lett., **69**, 648 (1992). DOI: 10.1103/PhysRevLett.69.648
[8] J. Wang, T.A. Arias, J.D. Joannopoulos, Phys. Rev. B, **47**, 10497 (1993). DOI: 10.1103/PhysRevB.47.10497
[9] Y. Segal, J.W. Reiner, A.M. Kolpak, Z. Zhang, S. Ismail-Beigi, C.H. Ahn, F.J. Walker, Phys. Rev. Lett., **102**, 116101 (2009). DOI: 10.1103/PhysRevLett.102.116101
[10] M. Kuzmin, P. Laukkanen, M.P.J. Punkkinen, M. Yasir, M. Tuominen, J. Dahl, J.J.K. Lång, J. Mäkelä, K. Kokko, Phys. Rev. B, **90**, 235405 (2014). DOI: 10.1103/PhysRevB.90.235405.
[11] J. Wang, M.R. Taaffe, INFORMS J. Comput., **27**, 193 (2015). DOI: 10.1287/ijoc.2014.0616
[12] Y. Li, K.-T. Fang, P. He, H. Peng, Mathematics, **10**, 3952 (2022). DOI: 10.3390/math10213952

Translated by EgoTranslating